Chinese Chemical Letters 34 (2023) 107738

Contents lists available at ScienceDirect

Chinese Chemical Letters

journal homepage: www.elsevier.com/locate/cclet

Synergetic treatment of oxygen microcapsules and lenvatinib for enhanced therapy of HCC by alleviating hypoxia condition and activating anti-tumor immunity

Jianpeng Sheng[a,b,c,1], Jiangchao Wu[a,b,c,1], Xianghong Yin[d,1], Zhu Sun[e], Xun Wang[a,b,c], Junlei Zhang[a,b,c], Jianghui Tang[a,b,c], Yongtao Ji[a,b,c], Jinyuan Song[a,b,c], Xiaobao Wei[a,b,c], Lin Wang[a,b,c], Yaxing Zhao[a,b,c], Hui Zhang[a,b,c], Taohong Li[a,b,c], Qi Zhang[a,b,c], Xueli Bai[a,b,c], Li Chen[e], Dong Chen[e,f,*], Tingbo Liang[a,b,c,*]

[a] Department of Hepatobiliary and Pancreatic Surgery, the First Affiliated Hospital, School of Medicine, Zhejiang University, Hangzhou 310002, China
[b] Zhejiang Provincial Key Laboratory of Pancreatic Disease, the First Affiliated Hospital, School of Medicine, Zhejiang University, Hangzhou 310002, China
[c] Zhejiang University Cancer Center, Zhejiang University, Hangzhou 310002, China
[d] School of Basic Medical Sciences, Institute of Hypoxia Medicine, Wenzhou Medical University, Wenzhou 325035, China
[e] College of Energy Engineering and State Key Laboratory of Fluid Power and Mechatronic Systems, Zhejiang University, Hangzhou 310027, China
[f] Department of Medical Oncology, the First Affiliated Hospital, School of Medicine, Zhejiang University, Hangzhou 310003, China

ARTICLE INFO

Article history:
Received 28 March 2022
Revised 4 August 2022
Accepted 8 August 2022
Available online 10 August 2022

Keywords:
Hypoxia
Oxygen microcapsules
Lenvatinib
Immune
Hepatocellular carcinoma

ABSTRACT

Hypoxia is a typical characteristic of hepatocellular carcinoma (HCC), which causes tremendous obstacles to tumor treatments. Current first-line treatment may further deteriorate tumor hypoxia. For example, Lenvatinib, a receptor tyrosine kinase inhibitor (RTKI), suppresses tumor growth *via* blocking vascular endothelial growth factor (VEGF) signaling, and can also inhibit angiogenesis, thus limiting oxygen supply to tumor sites. Therefore, alleviating tumor microenvironment (TME) hypoxia holds great potential for enhancing the therapeutic effect of RTKI. Here, nanoparticle-stabilized oxygen microcapsules, a stable and biocompatible oxygen-loaded delivery system, are successfully prepared through interfacial polymerization of polydopamine nanoparticles. The microcapsules with a large loading capacity of oxygen in the core show excellent bioavailability and dispersity, which could effectively improve the hypoxic TME when they serve as oxygen delivery vehicles. Synergetic treatments of Lenvatinib and oxygen microcapsules could induce the transition of "cold tumor" in an immune-suppressed state to "hot tumor" in an immune-activated state by improving tumor hypoxic TME and reducing angiogenesis in HCC. It is revealed that combined treatments of oxygen microcapsules and Lenvatinib could polarize tumor-associated macrophages (TAMs) to anti-tumor M1 cells and activate T cell-mediated anti-tumor immune responses. The results suggest that synergetic therapy using oxygen microcapsules and Lenvatinib could alleviate the hypoxic TME and enhance the therapeutic performance of RTKI, demonstrating a promising anti-tumor strategy for enhanced therapy of HCC.

Hepatocellular carcinoma (HCC), which causes a worldwide morbidity of 10 cases per 100,000 population per year [1], has been recognized as one of the most common malignant tumors in globe. HCC could be induced by various risk factors, such as hepatitis C virus (HCV), aflatoxin B1, undue alcohol consumption, hepatitis B virus (HBV), nonalcoholic fatty liver disease, hemochromatosis [1,2]. Various therapeutic treatments are developed to suppress the progression and establishment of HCC, and drug therapy (tyrosine kinase inhibitors including sorafenib, lenvatinib and regorafenib) has shown proven survival benefits.

Lenvatinib, for example, approved by FDA as the first-line therapy for cancerous patients with unresectable liver cancer, is an oral multi-kinase inhibitor, which blocks VEGF signaling and demonstrates antiangiogenic characteristics [3]. Angiogenesis inhibitors are considered to cause hypoperfusion in malignant tumor microenvironment (TME), thus reducing nutrient supply to tumor cells and limiting tumor growth [4,5]. However, the treatment of

* Corresponding authors.
E-mail addresses: chen_dong@zju.edu.cn (D. Chen), liangtingbo@zju.edu.cn (T. Liang).
[1] These authors contributed equally to this work.

https://doi.org/10.1016/j.cclet.2022.08.018
1001-8417/

Lenvatinib can also induce hypoxia in the TME of HCC by inducing hypoperfusion, which may reduce the efficacy of Lenvatinib. In addition, hypoxia is a typical characteristic of HCC due to the malformed blood vessels [6,7], and is known to result in resistance of anti-tumor therapy through many intracellular signaling pathways in autophagy, apoptosis, DNA damage, drug efflux, mitochondrial activity and p53 [8]. Therefore, intratumoral hypoxia affects HCC behaviors, such as cell proliferation, differentiation, apoptosis, genetic instability, tumor metabolism, vascularization/angiogenesis, immunosuppression, metastasis [9], and promotes the expression and stabilization of hypoxia-inducible factors, which play a crucial part in dampening anti-tumor therapies against HCC [10,11]. To solve the problem, combined treatments using Lenvatinib and specific strategy that can reverse the hypoxia in TME hold a great potential for HCC therapy.

Oxygen only has a very low solubility in water and it is difficult to deliver oxygen by intravenous injection. Microcarriers with small size, large specific surface area and outstanding bioavailability are excellent delivery vehicles to safely and effectively deliver oxygen [12,13], and many efforts have been dedicated to develop oxygen microcarriers to ameliorate the hypoxia of TME [14,15]. However, oxygen microbubbles stabilized by surfactant molecules are unstable and prone to coalescence [16,17]. Therefore, the design of oxygen microcarriers with excellent bioavailability, good dispersity in water and large loading capacity to realize ample oxygen supply into tumor sites remains a great challenge. Combined therapy of Lenvatinib and oxygen microcarriers remains unexplored in HCC.

Here, we develop a facile method to prepare nanoparticle-stabilized oxygen microcapsules, which load oxygen in the core of polydopamine nanoparticle shell. The oxygen microcapsules show excellent bioavailability *in vitro* and *in vivo* and are stable in water, which serve as good delivery vehicles to relieve the hypoxic microenvironment of HCC. Combined treatments of oxygen microcapsules and Lenvatinib demonstrate a powerful synergetic therapeutic effect by activating anti-tumor immunity. The synergetic therapy using oxygen microcapsules and Lenvatinib could polarize TAMs to anti-tumor M1 cells and activate T cell-mediated tumor cytotoxicity in HCC, which is promising anti-tumor strategy for enhanced therapy of HCC.

Polydopamine nanoparticles, which are prepared by interfacial polymerization, play an important role in stabilizing the oxygen microcapsules, as shown in the left of Fig. 1. Chitosan, polylysine and dopamine are first dissolved in an alkaline solution. When oxygen is blown into the solution and sheared into microbubbles, dopamine polymerizes into polydopamine nanoparticles at the water/oxygen interface. The polymerization of dopamine is expedited with the help of amino-rich polylysine and chitosan, which restrain the peroxidatic reaction of polydopamine nanoparticles and generate uniform polydopamine nanoparticles. In addition, amino-rich polylysine and chitosan provide sufficient active catechol groups to interact with polydopamine nanoparticles. Finally, stabilized oxygen microcapsules are achieved by cross-linking polydopamine nanoparticles with the help of glutaraldehyde at the water/oxygen interface and used as oxygen delivery vehicles with Lenvatinib for enhanced drug therapy of HCC, as schematically shown in the right of Fig. 1.

The oxygen microcapsules are stabilized by polydopamine nanoparticles to prevent coalescence and Ostwald ripening, as shown in Fig. 2A. The oxygen microcapsules could well disperse in water and show a high contrast edge under an optical microscope due to the mismatch in refractive indices between water and oxygen, as shown in Fig. 2B. When the oxygen microcapsules are dried in air and the oxygen cores are removed, the thin shells of collapsed oxygen microcapsules are revealed by the SEM image shown in Fig. 2C. Since polydopamine nanoparticles show a weak fluorescence, the core-shell microstructure of the oxygen microcapsules with an oxygen core and a thin shell of polydopamine nanoparticles is further verified by images from fluorescence confocal microscope, as the fluorescent, bright-filed and overlay images of oxygen microcapsules are shown from left to right in Fig. 2D, in which the shell of polydopamine nanoparticles shows weak fluorescent properties at the periphery of oxygen microcapsules when excited by the wavelength of 480 nm and detected between 507 nm and 673 nm. The thin-shell oxygen microcapsules can effectively parcel oxygen in the core and prevent the coalescence between oxygen microcapsules. The size of the oxygen microcapsules is roughly 5.3 ± 0.4 μm, as shown in Fig. 2E and Fig. S1A (Supporting information). Due to the presence of positively-charged polylysine and chitosan on the surface, the oxygen microcapsules have an average zeta potential of 50 ± 4 mV, as shown in Fig. 2F and Fig. S1B (Supporting information), which facilitates the dispersion of oxygen microcapsules in water. Moreover, oxygen microcapsules can also remain stable and well dispersed in PBS buffer with 10% fetal bovine serum (FBS), as shown in Fig. S2 (Supporting information), and more details of the preparation and characterization of oxygen microcapsules are described in Supporting information.

Since oxygen concentration in the oxygen microcapsules is higher than that in air, oxygen will gradually diffuse out of the microcapsules and the microcapsules will eventually collapse over time, as shown in Fig. 3A, which is different from the manner of responsive release. Oxygen microcapsules are preeminent carriers for oxygen delivery. When oxygen microcapsules are added to deoxygenated PBS buffer, oxygen could quickly diffuse into the PBS buffer under the driving force of oxygen concentration gradient, thus quickly increasing the oxygen concentration in the medium, as shown in Fig. 3B. For example, when 1 mL, 2 mL or 3 mL dispersion of oxygen microcapsules is added into 10 mL of deoxygenated PBS buffer, the oxygen concentration reaches a saturated value of 7 mg/L within approximately 37 min, 24 min or 20 min, respectively. To monitor the decrease of oxygen concentration in a nitrogen environment, the above-mentioned oxygen-saturated solutions with different amounts of oxygen microcapsules are placed in a nitrogen environment with nitrogen blowing on the surface. As oxygen diffuses into water and is continuously carried away by the nitrogen flow, the oxygen concentration in the solution will gradually decrease to 0 mg/L at 72 h, 84 h and 96 h for 1 mL, 2 mL and 3 mL dispersion of oxygen microcapsules, respectively, as shown in Fig. 3C. Therefore, the above results suggest that polydopamine-nanoparticle-stabilized oxygen microcapsules are excellent oxygen delivery vehicles.

Lenvatinib is a multi-kinase inhibitor with a preferential anti-angiogenic activity, which can cause tumor blood vessels to contract and reduce blood flow, limiting the supply of nutrients to tumor sites and thus suppressing tumor growth. However, the suppression of angiogenesis by Lenvatinib will also result in lack of oxygen in the TME. Hypoxia in solid tumors could in turn induce *in vivo* angiogenesis, thus reducing the efficacy of Lenvatinib [18,19]. In addition, hypoxia is known to be associated with the failures of many chemotherapy [20–22]. Therefore, oxygen microcapsules are expected to improve hypoxic condition in HCC and thus enhance the therapeutic efficacy of Lenvatinib. To test the hypothesis, sixteen C57BL/6 male mice are randomly divided into four groups: the first group receiving no therapy as the control group (C group), the second group receiving oxygen microcapsules (O group), the third group receiving Lenvatinib (L group) and the fourth group receiving combined treatments of Lenvatinib and oxygen microcapsules (L + O group), and detailed experimental procedures and characterization of the animal treatments are provided in Supporting Information. Animal experiments were approved by the Animal Care and Medical Ethics Committee of the First Affiliated Hospital, Zhejiang University. From the 6^{th} day, Hepa1–6 tumor-bearing

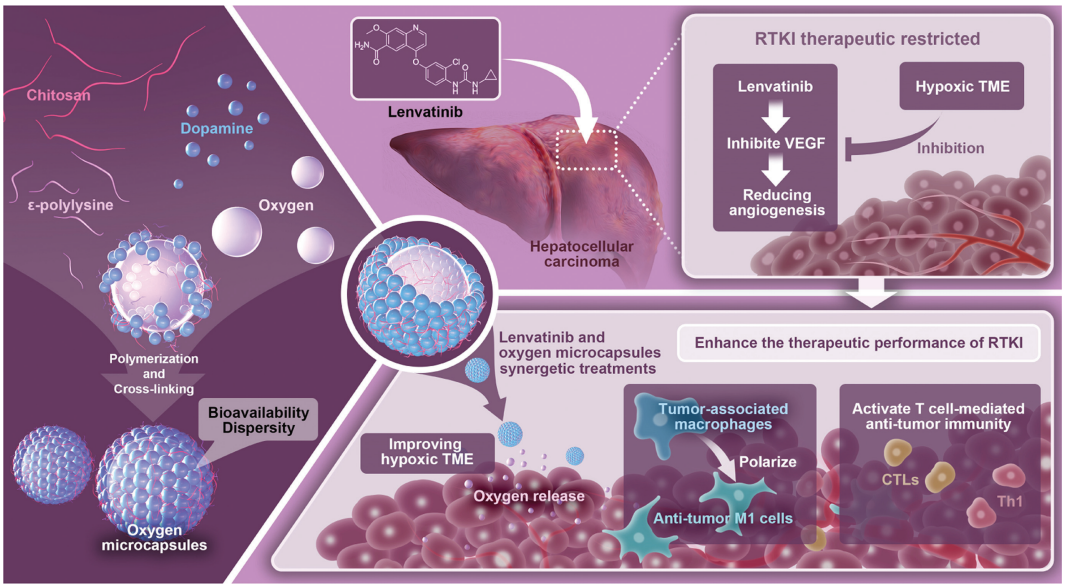

Fig. 1. Combined treatments of oxygen microcapsules and Lenvatinib by improving hypoxia in tumor microenvironment and activating anti-tumor immunity. Oxygen microcapsules are prepared by interfacial polymerization and stabilized by polydopamine nanoparticles.

mice are treated with intra-tumoral injection of PBS or oxygen microcapsules every two days for a total of 6 times; meanwhile, the mice are orally treated with 10 mg/kg/day of Lenvatinib for 10 consecutive days, as shown in Fig. 4A. After 11 days' treatments, no difference in body weight is observed between control group and groups under other different treatments, suggesting that mice are tolerated with oxygen microcapsules and Lenvatinib, as shown in Fig. 4B. However, photographs of dissected tumors show distinct difference in tumor size between control group and groups under different treatments, especially the L + O group under combined treatments showing the smallest tumor size, as shown in Fig. 4C. The differences are further confirmed by quantitative measurements of the tumor volume and tumor weight, as shown in Figs. 4D and E, respectively. Overall, the O group shows a little anti-tumor effect compared with the C group, while the L and L + O group can significantly suppress the tumor growth. The degree of tumor inhibition in the L + O group is obviously higher than that of the other groups, indicating enhanced therapeutic efficacy of combined treatments for HCC.

To investigate the underlying mechanism for the enhanced efficacy of the L + O group, the expression of hypoxia-inducible factor-1α (HIF-1α) in the TME is detected by immunohistochemistry, as shown in Fig. 5A. HIF-1α is a major transcription factor involved in the hypoxia response of HCC cells and its expression can reflect the degree of hypoxia in the TME [8,23-25]. Histological examinations of dissected tumors show that the expression of HIF-1α in the O and L + O groups is considerably lower than that in the other two groups, suggesting that intra-tumoral injection of oxygen microcapsules could effectively improve the hypoxia of TME. The improvement of hypoxic condition is further verified by analyzing hypoxic tumor cells (dead dye$^-$CD45$^-$EPCAM$^+$) in the TME using flow cytometry, as shown in Fig. 5B. Hypoxic EPCAM$^+$ tumor cells are significantly reduced in the O and L + O groups, which is consistent with the results of HIF-1α.

Angiogenesis, the formation of new blood vessels from the endothelium of existing vasculatures, is a critical factor for tumor growth and metastasis [26,27]. CD31$^+$, which is usually expressed in both differentiated and undifferentiated endothelial cells, is an indicator of tumor angiogenesis [28] and thus its expression is detected by flow cytometry to evaluate tumor angiogenesis, as shown in Figs. 5C and D. The lowest expression of CD31$^+$ observed in the L + O group suggests that oxygen microcapsules could assist Lenvatinib in reducing angiogenesis, as shown in Fig. 5E.

Previous studies suggest that hypoxia in the TME can lead to the formation of immunosuppressive microenvironment in HCC, which promotes immune evasion and tumor progression. For example, tumor-associated TAMs will polarize to either M1 cells, which are important for anti-tumor activity, or M2 cells, which play a crucial role in tumor promotion [29,30]. Hypoxia is known to result in recruitment and stimulation of immune-suppressor cells, such as M2 TAMs [31], and reduction of T cell infiltration [32]. Since oxygen microcapsules could effectively change the hypoxic TME, oxygen microcapsules are expected to promote immune activation in HCC and thus increase M1 TAMs and T cells in the TME.

To confirm the promoted immune activation in HCC by combined treatments of oxygen microcapsules and Lenvatinib, CD45$^+$ lymphocytes, TAMs (CD11b$^+$F4/80$^+$ in CD45$^+$), M1 TAMs (dead-dye$^-$CD45$^+$CD11b$^+$F4/80$^+$CD86$^+$CD206$^-$), M2 TAMs (dead-dye$^-$CD45$^+$CD11b$^+$F4/80$^+$CD86$^-$CD206$^+$), CD3$^+$ T cells, cytotoxic T lymphocytes (CTLs) and T helper 1 (Th1) lymphocytes in the tumor microenvironment are analyzed in detail using flow cytometry. The gating strategies for TAMs, M1 and M2 are demonstrated in Fig. 6A. The ratio of CD45$^+$ lymphocytes in the tumor microenvironment shows a remarkable increase in the L + O group as compared to the other groups, as shown in Fig. 6B. Though there is little difference in the ratio of TAMs between different groups (Fig. 6C), there are statistically significant differences in the ratios of TAM M1 and M2 subsets, as shown in Figs. 6D and E. As expected, the L + O group shows the highest ratio of M1 cells and the lowest ratio of M2 cells, when compared to the other groups. These results suggest that combined treatments of oxygen microcapsules could indeed promote immune activation in HCC and polarize TAMs towards M1 cells.

Similarly, T cell-mediated anti-tumor immunity in the TME are analyzed and the gating strategies for Th1 cells and CTLs are schematically shown in Fig. 7A. In general, higher ratios of Th1 cells and CTLs suggest a higher T cell-mediated anti-tumor immunity [33,34]. The results show that there are no significant differences in the ratios of CD3$^+$, CD8$^+$ and CD4$^+$ T cells between different groups, as shown in Figs. 7B-D, respectively. In contrast, the observed ratios of Th1 cells (CD45$^+$CD3$^+$CD4$^+$CD69$^+$)

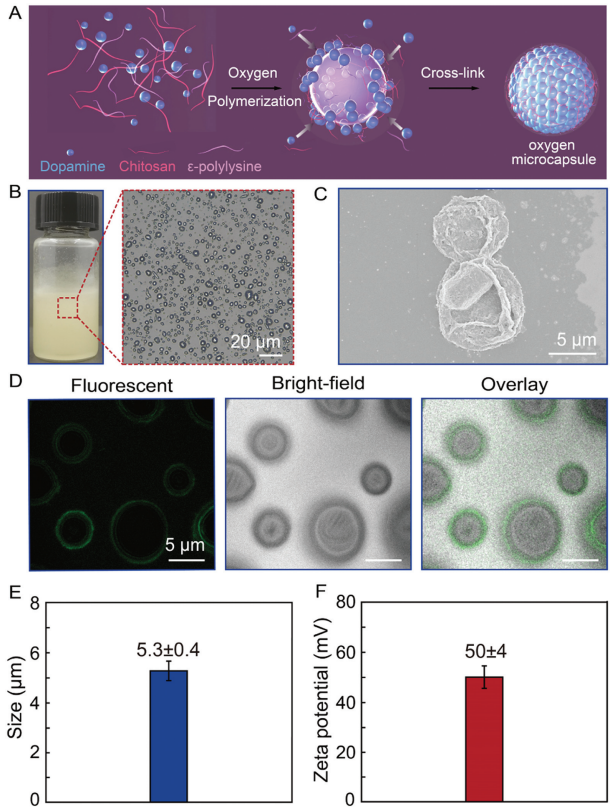

Fig. 2. Characterization of polydopamine-nanoparticle-stabilized oxygen microcapsules. (A) Schematics showing polydopamine-nanoparticle-stabilized oxygen microcapsules. (B) Dispersion of oxygen microcapsules in water. (C) SEM image of collapsed oxygen microcapsules showing ultra-thin shells. (D) Fluorescent, bright-filed, and overlay images of oxygen microcapsules. The shell of polydopamine nanoparticles shows weak fluorescent properties at the periphery of oxygen microcapsules. (E) Size distribution of oxygen microcapsules. (F) Zeta potential of oxygen microcapsules.

and CTLs ($CD45^+CD3^+CD8^+CD69^+$) in the L + O group are significantly higher than those in the other groups, as shown in Figs. 7E and F. Therefore, combined treatments of oxygen microcapsules and Lenvatinib could induce strong adaptive T cell-mediated anti-tumor immunity.

Histological examinations of dissected tumors under different treatments using Ki67 and TUNEL assays show that combined treatments of oxygen microcapsules and Lenvatinib contain the least proliferative markers (labeled by Ki67) and highest apoptosis index (labeled by TUNEL) compared with the other groups, suggesting most apoptosis and least proliferation, as shown in Fig. 7G. These results suggest that improving hypoxic TME using oxygen microcapsules can help to polarize TAMs towards M1 cells and activate T cell-mediated anti-tumor immune responses.

Polydopamine-nanoparticle-stabilized oxygen microcapsules are expected to possess good biocompatibility, since previous studies have suggested that polydopamine, a biocompatible polymer, is a promising carrier for loading different anticancer drugs for cancer treatments [35–37]. To further evaluate the biosafety of oxygen microcapsules, tissues from major organs of mice under different treatments, including heart, liver, spleen, lung and kidney, are examined by histopathological examinations, as shown in Fig. 8. The H&E stained micrographs show no observable tissue damage and no observable difference in the C, L, O and L + O groups. The results are consistent with the previous discussions that there is no significant weight loss in the mice under different treatments. Therefore, combined treatments of oxygen microcapsules and Lenvatinib is a promising therapeutic strategy for enhanced cancer therapy.

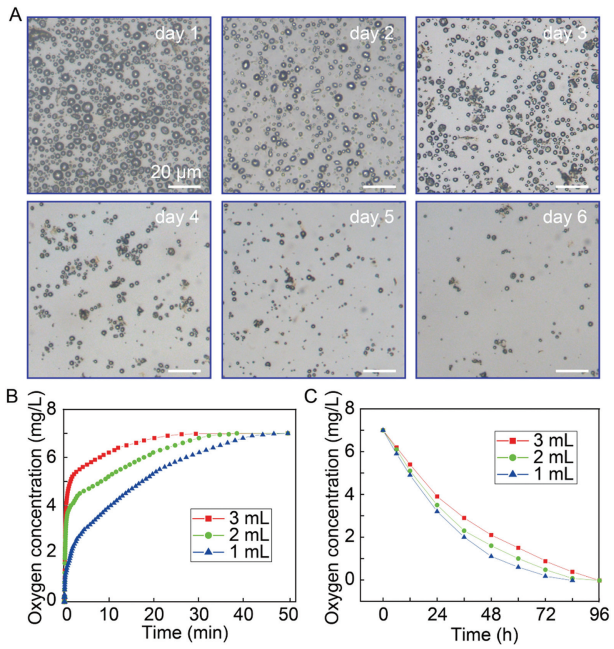

Fig. 3. Oxygen delivery performances of polydopamine-nanoparticle-stabilized oxygen microcapsules. (A) Optical images of oxygen microcapsules exposed in air over time. The interval between neighboring images is 1 day. As oxygen is gradually released, oxygen microcapsules shrink and collapse. (B) Increase of oxygen concentration over time when 1 mL, 2 mL and 3 mL dispersions of oxygen microcapsules are added into in 10 mL deoxygenated PBS buffer, respectively. PBS is deoxygenated by nitrogen purge. The concentration of oxygen microcapsule dispersions is roughly 1 mL oxygen microcapsules in 1 mL water. (C) Release of oxygen from oxygen microcapsule dispersions over time in a nitrogen environment with nitrogen blowing on the surface.

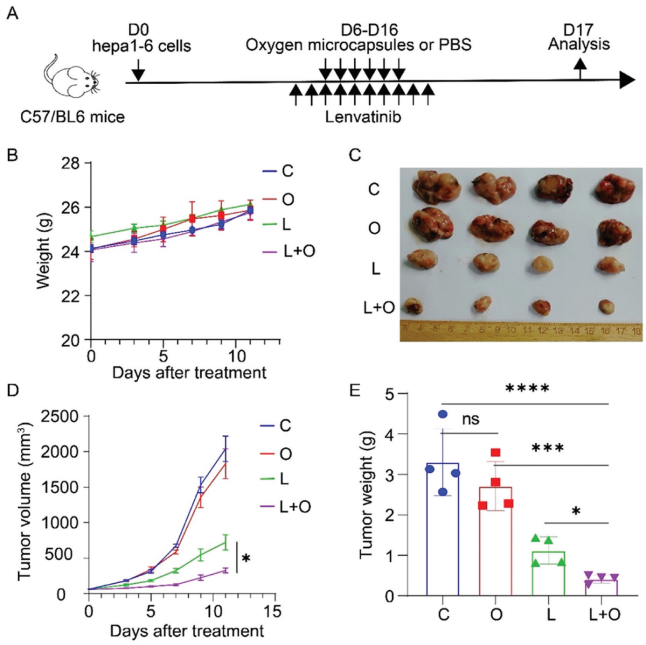

Fig. 4. Synergetic therapy using oxygen microcapsules and Lenvatinib *in vivo*. (A) Therapeutic schedule for Hepa1–6 tumor-bearing mice using combined treatments of oxygen microcapsules and Lenvatinib. (B) Body weights of mice under different treatments over time. (C) Photograph of dissected tumors under different therapies. (D) Tumor volumes of mice under different therapies at different times. (E) Changes of tumor weight over time in different groups. Data are shown as mean ± SEM ($n = 4$ per group). If not specified, C group: Control group; O group: Oxygen microcapsule therapy; L group: Lenvatinib therapy; L + O group: Combination therapy of Lenvatinib and oxygen microcapsules. If not specified, $^*P < 0.05$; $^{**}P < 0.01$; $^{***}P < 0.001$; $^{****}P < 0.0001$; ns: no significance.

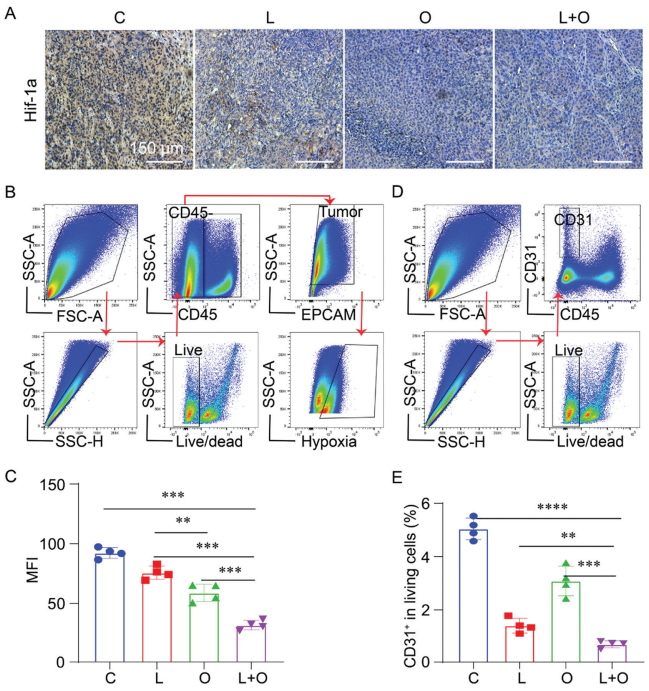

Fig. 5. Improvement of hypoxia and reduction of angiogenesis *in vivo* using combined treatments of oxygen microcapsules and Lenvatinib. (A) The expression of HIF-1α in different groups by histological examinations. (B) Gating strategy for hypoxic tumor cells (dead dye$^-$CD45$^-$EPCAM$^+$). (C) Mean fluorescent intensity (MFI) of hypoxic tumor cells under different therapies. (D) Gating strategy for CD31 (dead dye$^-$CD45$^-$CD31$^+$) in the TME. (E) Proportions of CD31 under different treatments. Data are shown as the mean ± SEM ($n = 4$ per group). Data are shown as the mean ± SEM ($n = 4$ per group). $^{**}P < 0.01$; $^{***}P < 0.001$; $^{****}P < 0.0001$.

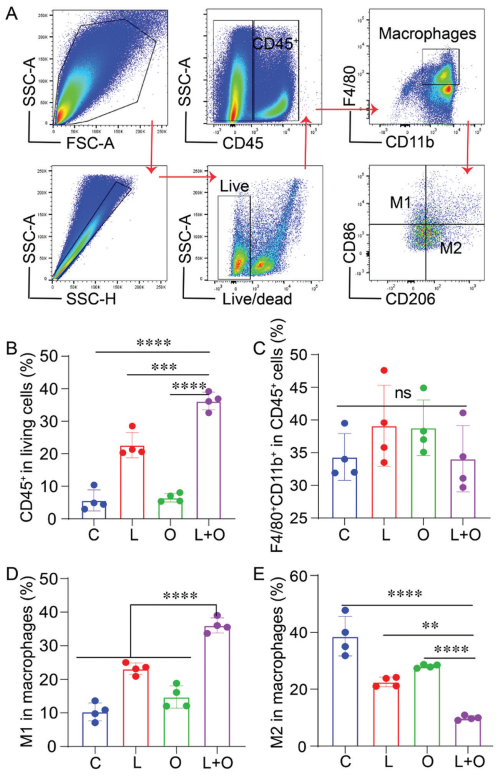

Fig. 6. Macrophage-mediated immune activation under combined treatments of oxygen microcapsules and Lenvatinib. (A) Gating strategy for macrophages (TAMs), M1 and M2 in the tumor microenvironment by flow cytometry. Proportions of (B) CD45$^+$ lymphocytes, (C) TAMs, (D) M1 and (E) M2 in the TME under different treatments. Data are presented as mean ± SEM ($n = 4$ per group). $^{**}P < 0.01$; $^{***}P < 0.001$; $^{****}P < 0.0001$; ns: no significance.

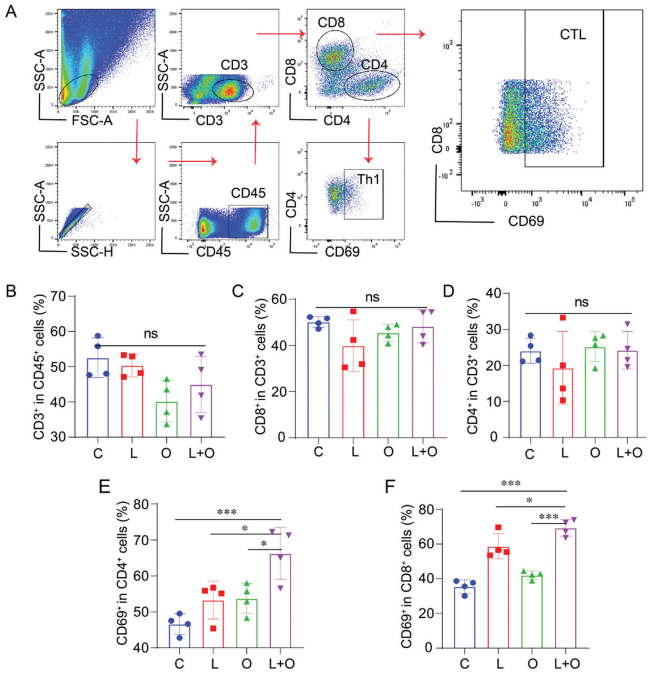

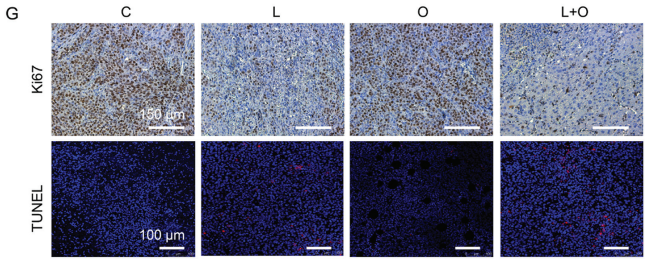

Fig. 7. T cell-mediated immune activation of oxygen microcapsules under combined treatments of oxygen microcapsules and Lenvatinib. (A) Gating strategy for T helper 1 (Th1) cells and cytotoxic T lymphocytes (CTLs) by flow cytometry. Percentages of (B) CD3$^+$ T cells, (C) CD8$^+$ T cells, (D) CD4$^+$ T cells, (E) CTLs and (F) Th1 cells within the TME of each group. Data are presented as the mean ± SEM ($n = 4$ per group). $^*P < 0.05$; $^{***}P < 0.001$; ns: no significance. (G) Histological examinations of dissected tumors under different treatments using Ki67 and TUNEL assays.

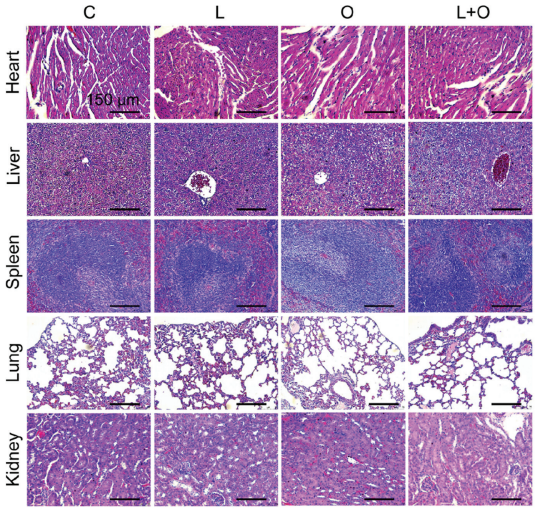

Fig. 8. Safety evaluation of combined treatments of oxygen microcapsules and Lenvatinib. H&E stained micrographs of major organs, including heart, liver, spleen, lung and kidney, from mice under different treatments. No significant differences are observed between control group and groups under other treatments.

Hypoxia in the tumor microenvironment is a big obstacle for anti-tumor therapy and it causes resistance of anti-tumor drugs for hepatocellular carcinoma treatments by HIF-1α, autophagy and so on [38]. To improve the hypoxic TME, nanoparticle-stabilized oxygen microcapsules consisting of an oxygen core and a shell of polydopamine nanoparticles are prepared *via* interfacial polymerization. The microcapsules possess advantages of excellent bioavailability, high loading capacity, good dispersity in water and high stability against coalescence, being outstanding oxygen delivery vehicles. Combined treatments of oxygen microcapsules and Lenvatinib are proved to significantly improve the hypoxia in the TME and enhance the anti-tumor performance for HCC *in vivo*. Details analysis of the ratio of cells in the TME suggests that synergetic therapy using oxygen microcapsules and Lenvatinib could polarize TAMs to anti-tumor M1 cells and activate T cell-mediated anti-tumor immune responses. Therefore, combined treatments of oxygen microcapsules and Lenvatinib provide an important example for enhanced therapy of HCC. The synergic strategy could be extended to other tumors and oxygen microcapsules, which could effectively improve the hypoxic TME, are applicable in many scenarios.

Declaration of competing interest

The authors declare that they have no known competing financial interests or personal relationships that could have appeared to influence the work reported in this paper.

Acknowledgments

This work was supported by the National Key Research and Development Program of China (Nos. 2019YFA0803000, 2019YFC1316000), the National Natural Science Foundation of China (Nos. U20A20378, 21878258), Zhejiang Provincial Natural Science Foundation of China (No. Y20B060027) and Scientific Research Fund of Zhejiang Provincial Education Department (No. Y202045652).

Supplementary materials

Supplementary material associated with this article can be found, in the online version, at doi:10.1016/j.cclet.2022.08.018.

References

[1] A. Villanueva, N. Engl. J. Med. 380 (2019) 1450–1462.
[2] N. Personeni, T. Pressiani, L. Rimassa, J. Hepatocell. Carcinoma 6 (2019) 31–39.
[3] A. Nair, K. Reece, M.B. Donoghue, et al., Oncologist 26 (2021) e484–e491.
[4] N. Une, M. Takano-Kasuya, N. Kitamura, et al., Med. Oncol. 38 (2021) 60.
[5] M.W. Dewhirst, Y. Cao, B. Moeller, Nat. Rev. Cancer 8 (2008) 425–437.
[6] J. Fu, T. Li, Y. Yang, et al., Biomaterials 268 (2021) 120537.
[7] B. Wang, Q. Zhao, Y. Zhang, et al., J. Exp. Clin. Cancer Res. 40 (2021) 24.
[8] X. Jing, F. Yang, C. Shao, et al., Mol. Cancer 18 (2019) 157.
[9] C. Wigerup, S. Påhlman, D. Bexell, Pharmacol. Ther. 164 (2016) 152–169.
[10] V.W.H. Yuen, C.C.L. Wong, J. Clin. Investig. 130 (2020) 5052–5062.
[11] Z. Mo, D. Liu, D. Rong, S. Zhang, Front. Immunol. 12 (2021) 611058.
[12] X. Dai, J. Ruan, Y. Guo, et al., Chem. Eng. J. 422 (2021) 130109.
[13] Z. Sun, C. Yang, M. Eggersdorfer, et al., Chin. Chem. Lett. 31 (2020) 249–252.
[14] A. Sharma, J.F. Arambula, S. Koo, et al., Chem. Soc. Rev. 48 (2019) 771–813.
[15] R.M. Phillips, Cancer Chemother. Pharmacol. 77 (2016) 441–457.
[16] Z. Sun, C. Yang, F. Wang, et al., Angew. Chem. Int. Ed. 59 (2020) 9365–9369.
[17] Z. Sun, B. Wu, Y. Ren, et al., ChemPlusChem 86 (2021) 49–58.
[18] D. Liao, R.S. Johnson, Cancer Metastasis Rev. (2007) 281–290.
[19] B. Muz, P. de la Puente, F. Azab, A.K. Azab, Hypoxia (Auckl) 3 (2015) 83–92.
[20] O. Tredan, C.M. Galmarini, K. Patel, I.F. Tannock, J. Natl. Cancer Inst. 99 (2007) 1441–1454.
[21] E. Tak, S. Lee, J. Lee, et al., J. Hepatol. 54 (2011) 328–339.
[22] B. Wu, Z. Sun, J. Wu, et al., Angew. Chem. Int. Ed. 60 (2021) 9284–9289.
[23] H. Choudhry, A.L. Harris, Cell Metab. 27 (2018) 281–298.
[24] J. Zhang, Q. Zhang, Y. Lou, et al., Hepatology 67 (2018) 1872–1889.
[25] Y. Pan, X. Chen, L. Dong, et al., Chin. Chem. Lett. 32 (2021) 3895–3898.
[26] N. Nishida, H. Yano, T. Nishida, T. Kamura, M. Kojiro, Vasc. Health Risk Manag 2 (2006) 213–219.
[27] M. Rajabi, S. Mousa, Biomedicines 5 (2017) 34.
[28] J. Xing, W. He, Y.W. Ding, Y. Li, Y.D. Li, Med. Ultrason. 20 (2018) 37–42.
[29] L. Parisi, E. Gini, D. Baci, et al., J. Immunol. Res. 2018 (2018) 1–25.
[30] M. Oshi, Y. Tokumaru, M. Asaoka, et al., Sci. Rep. 10 (2020) 16554.
[31] A. Henze, M. Mazzone, J. Clin. Investig. 126 (2016) 3672–3679.
[32] P. Jayaprakash, M. Ai, A. Liu, et al., J. Clin. Investig. 128 (2018) 5137–5149.
[33] N. Gong, N.C. Sheppard, M.M. Billingsley, C.H. June, M.J. Mitchell, Nat. Nanotechnol. 16 (2021) 25–36.
[34] F. Meric-Bernstam, J. Larkin, J. Tabernero, C. Bonini, Lancet 397 (2021) 1010–1022.
[35] Z. Li, B. Wang, Z. Zhang, et al., Mol. Ther. 26 (2018) 1385–1393.
[36] S. Tavakoli, M. Kharaziha, S. Nemati, Nano-Struct. Nano-Objects 25 (2021) 100639.
[37] P. Zhang, Q. Xu, J. Du, Y. Wang, RSC Adv. 8 (2018) 34596–34602.
[38] C. Liang, Z. Dong, X. Cai, et al., Cell Death Dis. 11 (2020) 1017.